J Solid State Electrochem (2010) 14:1601–1608
DOI 10.1007/s10008-009-0993-0

ORIGINAL PAPER

Electrochemical corrosion behaviors and corrosion protection properties of Ni–Co alloy coating prepared on sintered NdFeB permanent magnet

Xiaokui Yang · Qing Li · Shiyan Zhang · Hui Gao · Fei Luo · Yan Dai

Received: 8 September 2009 / Revised: 6 November 2009 / Accepted: 14 December 2009 / Published online: 6 January 2010

Abstract In this study, a protective Ni–Co alloy coating was prepared on sintered NdFeB magnet applying electrodeposition technique. A pure nickel coating was also studied for a comparison. The microstructure, surface morphologies, and chemical composition of coatings were investigated using X-ray diffraction, scanning electron microscope, and energy dispersive spectroscopy, respectively. The corrosion protection properties of coatings for NdFeB magnet in neutral 3.5 wt.% NaCl solutions were evaluated by potentiodynamic polarization and electrochemical impedance spectroscopy (EIS) techniques. The microstructure and surface morphologies analysis showed that the addition of cobalt element into matrix metal Ni altered the preferential orientation of pure nickel coating from (2 0 0) crystal face for pure nickel coating to (1 1 1) crystal face for Ni–Co alloy coating, and made the surface morphologies more compact and uniform due to the grain-refining. The results of potentiodynamic polarization test showed that compared with pure nickel coating, Ni–Co alloy coating exhibited much nobler corrosion potential (E_{corr}) and lower corrosion current density (j_{corr}), indicating better anticorrosive properties. The long-term immersion test by dint of EIS indicated that the Ni–Co alloy coating still presented high impedance value of 1.9×10^5 Ω cm^2 with the immersion time of 576 h indicating the excellent anticorrosive properties, and corrosion protection properties of nickel coating for NdFeB magnet practically disappeared with the immersion time of 144 h, which also indicated that the Ni–Co alloy coating provided better corrosion protection properties for the NdFeB magnet compared with nickel coating.

Keywords NdFeB permanent magnet · Ni–Co alloy coating · Corrosion protection · Electrochemical corrosion behaviors · Electrochemical impedance spectroscopy

X. Yang
School of Materials Science and Engineering,
Southwest University,
400715 Chongqing, People's Republic of China

Q. Li (✉) · S. Zhang · H. Gao · F. Luo · Y. Dai
School of Chemistry and Chemical Engineering,
Southwest University,
400715 Chongqing, People's Republic of China
e-mail: liqingd@swu.edu.cn
e-mail: liqingswu@yeah.net

Introduction

The sintered NdFeB (neodymium-iron-boron) magnet, which was developed at the beginning of the 1980s, has been used for many applications in various fields such as acoustics, communications, and automation due to its excellent properties such as high remanence, high coercivity, and large energy product [1–3]. However, sintered NdFeB permanent magnet is highly vulnerable to the attack of corrosive environment due to the presence of the Nd-rich phase, which impedes and limits their extensive applications [4, 5].

In order to improve the corrosion resistance of sintered NdFeB magnet, numerous attempts have been made, such as alloy additions and surface treatment [6–20]. Within our knowledge, most of the researches mentioned above are focusing on the tests of the short-term anticorrosive properties of coatings or films [6–19] but seldom the tests of the long-term anticorrosive properties [20]. Of the two, the latter is far better than the former to reflect the actual corrosion protection properties of coatings or films for sintered NdFeB magnet. Electroplating of metal coatings, as a traditional surface treatment technique, has been brought for surface modification of many metals, such as Al, Fe,

NdFeB, and Mg. The electrodeposited Ni–Co alloy coating, which possesses good adhesion, high strength, good wear resistance, corrosion resistance, thermal stability, heat-conductive, and electrocatalytic activity properties [21–31], has attracted much attention. Unfortunately, most of these reports are focusing on the investigation on the preparation, electrocatalytic activity properties, and mechanical properties, etc.; however, little information on anticorrosive properties of Ni–Co alloy coating is available. Moreover, so far, no work has reported on the changes in the electrochemical corrosion behaviors and anticorrosive properties of Ni–Co alloy coating in the course of long-term immersion test which may be necessarily an indicator of a practically useful coating.

In this study, Ni–Co alloy coating was successfully applied to sintered NdFeB magnet. The main aim of this study is to understand the changes in the electrochemical corrosion behaviors and anticorrosive properties of Ni–Co alloy coating in neutral 3.5 wt.% NaCl solutions, which are the most adopted corrosive medium, and get some fundamental information on the feasibility of the long-term corrosion protection for NdFeB magnet.

Experimental details

Materials

The commercial powder-sintered NdFeB magnet for this investigation was purchased from Shenzhen (Dongsheng Magn. Mater. Co. Ltd., China). They were composed of 60.9 wt.% Fe, 28.6 wt.% Nd, 1.0 wt.% B, and other elements, and were in disk form with diameter and thickness of 12.0 and 2.0 mm, respectively. The nickel plate with the purity of 99.99 wt.% was used as anode on the side of the electrolytic cell.

Pretreatment of substrates

Before electrodeposition, the disk NdFeB magnet (substrate) was sequentially polished with silicon carbide paper from grit #400 to #2000, rinsed with deionized water, ultrasonically degreased in an alkaline solutions containing 70 g L^{-1} $Na_3PO_4{\cdot}12H_2O$, 50 g L^{-1} Na_2CO_3, 10 g L^{-1} NaOH, 0.5 g L^{-1} sodium dodecyl sulfate, and 0.5 g L^{-1} OP-10 (pH adjusted to 10~11 by formic acid) at 70 °C for 2 min, and then rinsed with hot and cold deionized water, respectively. In order to remove the oxide film on the surface of NdFeB magnet, the above pretreated NdFeB magnet was dipped into an acid solutions containing 40 mL L^{-1} HNO_3 (65.0 wt.%) and 0.5 g L^{-1} thiourea with the pH adjusted to 4~5 by ammonia, for approximately 10 s at room temperature. At last, the NdFeB magnet was activated by the anhydrous $PdCl_2$/EtOH solutions, with the $PdCl_2$ of 0.4 g L^{-1}, for 2~5 s at room temperature.

Electrodeposition process

Ni–Co alloy coating was prepared under direct current conditions. The optimized bath compositions and other parameters obtained from large numbers of orthogonal experiments are given in Table 1. Pure nickel coating was prepared in almost the same solutions mentioned above except the addition of $CoCl_2{\cdot}6H_2O$ under the same electrodeposition conditions.

Test

The phase structures of coatings were analyzed by X-ray diffractometer (XRD) (Beijing Purkinje general instrument Co. Ltd., China) operated at 36 kV and 20 mA with Cu K_a radiation. The average crystallite size was determined with reference to (1 1 1) and (2 0 0) crystal face using Scherrer equation.

The surface morphologies and compositions of coatings were studied using a scanning electron microscope (SEM; Model TESCAN VEGAIILMU, Czech) coupled with energy dispersive analyzer system (EDS).

The coating adhesion was evaluated according to ASTMB571 standard (heat quenching test, 220 °C aging treatment for 1 h, then water quenching at room temperature).

The electrochemical corrosion tests were carried out using a classical three-electrode cell with platinum as counter electrode, saturated calomel electrode (+0.242 V vs standard hydrogen electrode) as reference electrode, and the samples with an exposed area of 1 cm^2 as working electrode. The potentiodynamic polarization curves were performed by PS-268B system (Zhongfu, Beijing, China) with a constant voltage scan rate of 0.5 mV s^{-1}. The electrochemical impedance spectroscopy (EIS) measurements were performed with CS350 electrochemical workstation (Wuhan CorroTest Instrument Co. Ltd., China). The amplitude of sinusoidal signal employed was 5 mV, and the

Table 1 Bath compositions and operating conditions for electrodeposition

Bath compositions and operating conditions	Quantity
$NiSO_4{\cdot}6H_2O$	250 g L^{-1}
$CoCl_2{\cdot}6H_2O$	16 g L^{-1}
H_3BO_3	32 g L^{-1}
NaCl	12 g L^{-1}
Current density	5 A dm^{-2}
pH	3.6
Temperature	40 °C
Time	30 min

frequency range studied was from 10^5 to 10^{-2} Hz. The acquired data were curve fitted and analyzed using *ZsimpWin 3.10* software. The corrosive medium used for electrochemical corrosion tests was neutral 3.5 wt.% NaCl solutions, and the test temperature was maintained at 30 °C. All the electrochemical corrosion tests were normally at least repeated three times under the same conditions, checking that they presented reasonable reproducibility.

Results and discussion

XRD measurements

Figure 1a, b shows the XRD diffract patterns of pure nickel coating and Ni–Co alloy coating, respectively. It is apparent that pure nickel coating exhibited intense (2 0 0) preferred orientation, and Ni–Co alloy coating exhibited (1 1 1) preferential orientation, which indicated that the embedding of cobalt element in Ni matrix metal altered the preferential orientation from (2 0 0) crystal face for pure nickel coating to (1 1 1) crystal face for Ni–Co alloy coating. The average grain size of pure nickel coating and Ni–Co alloy coating was measured to be 47 and 35 nm, respectively, indicating the reduction of average crystallite size after the addition of cobalt element in Ni matrix metal. The peaks corresponding to Co phase was not found in the diffract patterns, which could be ascribed to the fact that crystal lattice in Ni matrix had been replaced by Co partly and formed solid solution [21].

SEM and EDS measurements

The surface morphologies of pure nickel coating and Ni–Co alloy coating are displayed in Fig. 2. Figure 2 illustrates

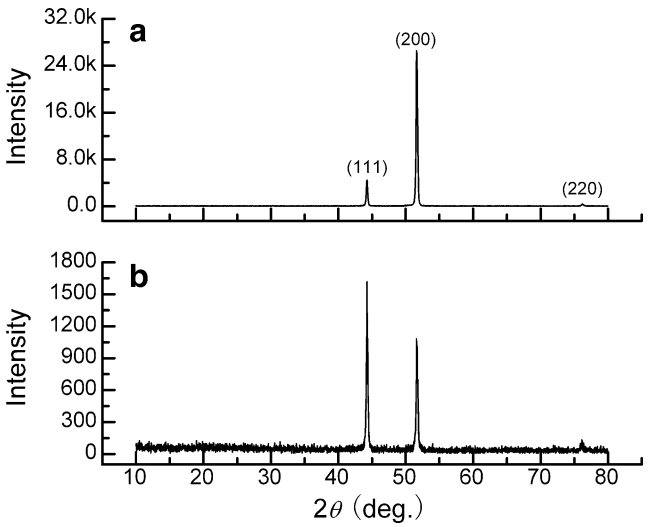

Fig. 1 X-ray diffraction patterns of pure nickel coating (**a**) and Ni–Co alloy coating (**b**)

that Ni–Co alloy coating presented more uniform and compact surface morphologies compared with pure nickel coating, and many raised grain congeries were observed in pure nickel coating, which may be attributed to the smaller average grain size for Ni–Co alloy coating compared with pure nickel coating. The EDS analysis of Ni–Co alloy coating indicated the existence of cobalt element in the alloy coating. In each EDS measurement, an area of 10 μm in diameter was examined to a depth of about 2 μm, and the measurements were at least repeated three times. The examinations showed that the content of Co in the alloy coatings amounted to 19–21 wt.%. According to the adhesion test, the phenomena of blisters and crackles were not found. Thus, the adhesion of between Ni–Co alloy coating and the NdFeB substrate was good. From the cross-section morphologies, as shown in Fig. 3, it can be seen that the thickness of Ni–Co alloy coating was approximately 25 μm, which was almost the same with that of pure nickel coating (not shown).

Potentiodynamic polarization test

The typical potentiodynamic polarization curves of different specimens are presented in Fig. 4.

Figure 4 shows that both pure nickel coating and Ni–Co alloy coating exhibited passive region, which indicated that anodic reaction was inhibited to a great extent with the increase of anodic potential. However, the passive region was not observed for NdFeB magnet which exhibited active dissolution without any distinctive transition to passivation within the range of anodic potential studied. With the increasing anodic potential, the anodic current densities significantly increased for NdFeB magnet, suggesting a fast anodic dissolution. It can be also seen from Fig. 4 that compared with pure nickel coating, Ni–Co alloy coating showed much lower anodic current densities suggesting lower corrosion rate.

Corrosion current density (j_{corr}) and corrosion potential (E_{corr}) were calculated from the polarization curves displayed in Fig. 4 using Tafel extrapolation. Ni–Co alloy coating exhibited the noblest E_{corr} with a value of −280 mV and the lowest j_{corr} with a value of 1.6×10^{-7} A cm^{-2}, while NdFeB magnet showed the lowest E_{corr} with a value of −756 mV and the highest j_{corr} with a value of 1.2×10^{-5} A cm^{-2}, which suggested that Ni–Co alloy coating could provide the best corrosion protection for the NdFeB magnet. The E_{corr} and j_{corr} of pure nickel coating were measured to be −381 mV and 1.1×10^{-6} A cm^{-2}, respectively.

From the analysis mentioned above, it can be seen that both Ni–Co alloy coating and pure nickel coating could provide corrosion protection for NdFeB magnet. Compared with pure nickel coating, Ni–Co alloy coating showed

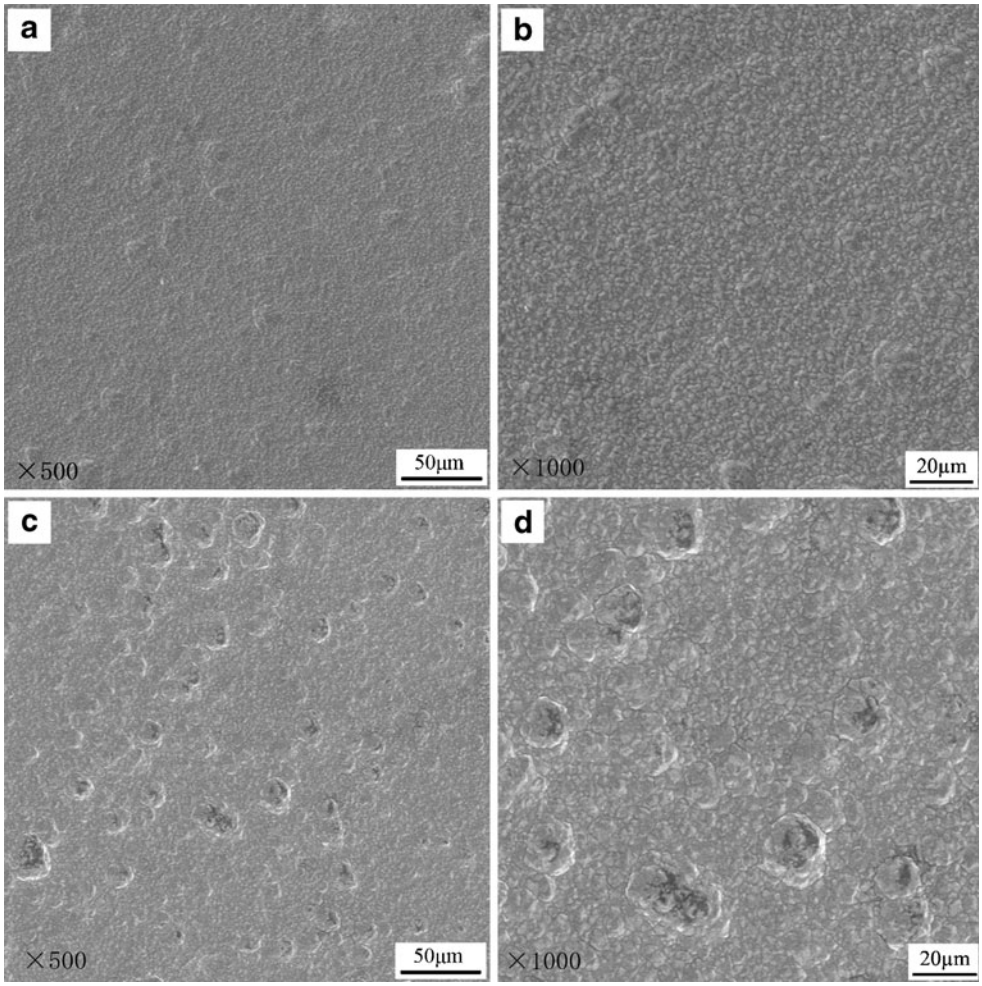

Fig. 2 Surface morphologies of Ni–Co alloy coating (**a**, **b**) and pure nickel coating (**c**, **d**)

much nobler E_{corr} and lower j_{corr} indicating better corrosion protection for NdFeB magnet, which could be attributed to more uniform and compact surface morphologies as well as the grain-refining for Ni–Co alloy coating.

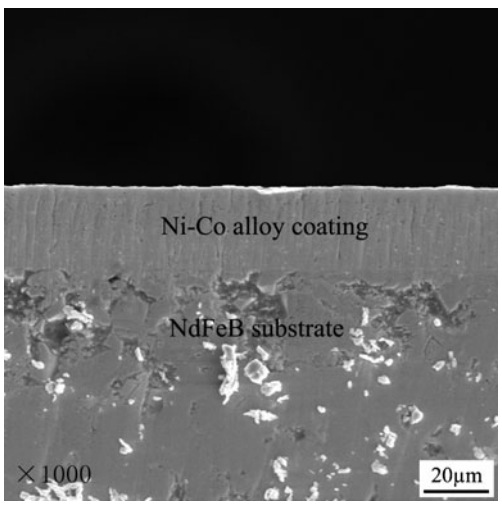

Fig. 3 Cross-section morphologies of Ni–Co alloy coating

Electrochemical impedance spectroscopy test

EIS is one of the most intensively used and powerful techniques for investigation and prediction of corrosion

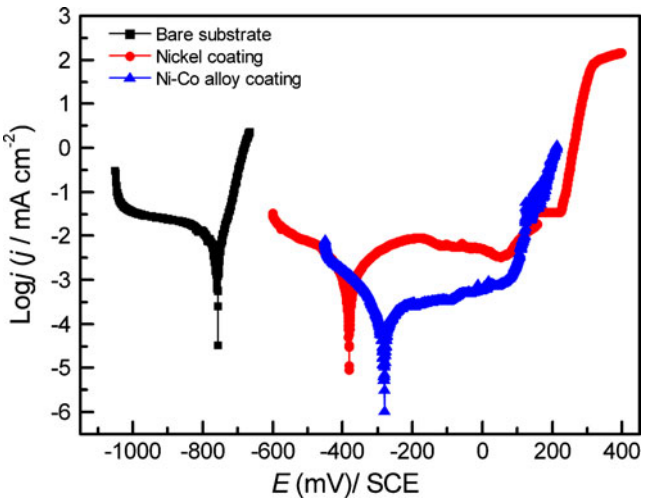

Fig. 4 Typical potentiodynamic polarization curves of different specimens

protection. EIS could provide indication of changes in coating and metal interface performance long before visual changes can be observed using traditional exposure test [32].

In this section, the evolution of electrochemical corrosion behaviors and corrosion protection properties of Ni–Co alloy coating for NdFeB magnet in the long-term immersion test are studied by dint of EIS. For a comparison, the changes in the electrochemical corrosion behaviors and corrosion protection properties of nickel coating for NdFeB magnet have been also described simply.

Figure 5 displays the typical Nyquist plot of bare NdFeB magnet (inserted plots), and the evolution of the impedance spectroscopy of pure nickel coating with different immersion times.

The Nyquist plot of bare NdFeB magnet (inserted plot) shows that the diagram was mainly composed of only one depressive loop over the whole frequency range corresponding to an active dissolution of NdFeB magnet.

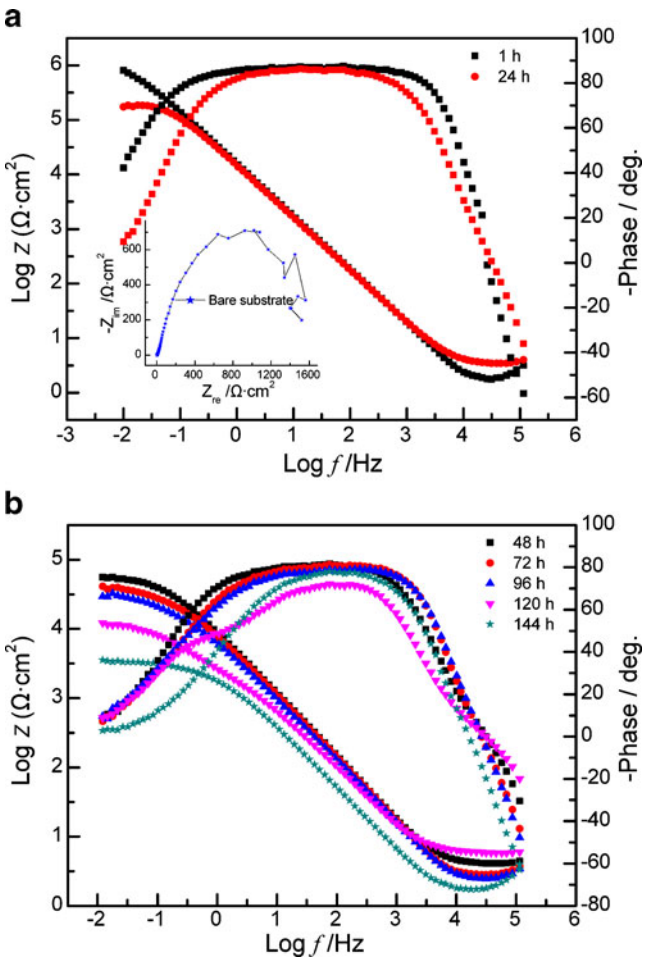

Fig. 5 Electrochemical impedance spectroscopy plots of pure nickel coating with different immersion times and NdFeB magnet (inserted plot)

Some scattered points were observed at low-frequency region indicating the instability of surface state of NdFeB magnet in the test process, which may be attributed to the fast corrosion process. The charge transfer resistance of bare NdFeB magnet was measured to be approximately 1,600 Ω cm^2, which could be estimated from the intersection of the semicircle with the real axis of the Nyquist diagram [32].

The Bode plots (impedance modulus |Z| as a function of frequency) of pure nickel coating indicate that impedance modulus |Z| continuously decreased with the increase in immersion time, especially the immersion time from 1 to 24 h, in which impedance modulus |Z| decreased approximately one order of magnitude. The decreasing impedance modulus |Z| indicated that the corrosion was gradually accelerated with the increase in immersion time and the corrosion protection properties of the nickel coating for NdFeB magnet decreased. With the immersion time of 144 h, from the impedance modulus |Z| at the lowest frequency, it can be seen that the impedance modulus |Z| of nickel coated NdFeB corrosion system had decreased to approximately $10^{3.5}$ Ω cm^2 (2,300 Ω cm^2). In addition, the brown rust was observed in the corrosion solutions, which indicated that the corrosion protection properties of nickel coating for NdFeB magnet practically disappeared.

The EIS plots of Ni–Co alloy coating with different immersion times in neutral 3.5 wt.% NaCl solutions are shown in Fig. 6. It can be seen from Nyquist plots (Fig. 6b, d) that the diameter of the capacitance loop of Ni–Co alloy coating fleetly increased with the initial immersion time from 1 to 48 h, suggesting the increase of impedance value, and then the impedance value decreased as the immersion time increased until the immersion time of 240 h. With the further increase of immersion time, the impedance value began to increase again. With the immersion time of 576 h, the impedance value still remained rather high, showing the excellent corrosion protection properties of Ni–Co alloy coating for NdFeB magnet. At the initial stage of immersion test, the increase in impedance value can be ascribed to the formation and growth of the passive film on the metal surface [17, 33–37]. With the increase of immersion time, the decrease in impedance value may have resulted from the fact that the passive film suffered from the attack of corrosive medium, e.g., chloride ions, resulting in the decrease in thickness and/or the increase in defect.

Fitting the EIS plots of Ni–Co alloy coating was attempted by different electrochemical equivalent circuits, taking into account the previous studies on the metal passive system [34–38]. The best agreement between experimental and fitting data was obtained with the equivalent circuit presented in Fig. 7. Two (RQ) parallel

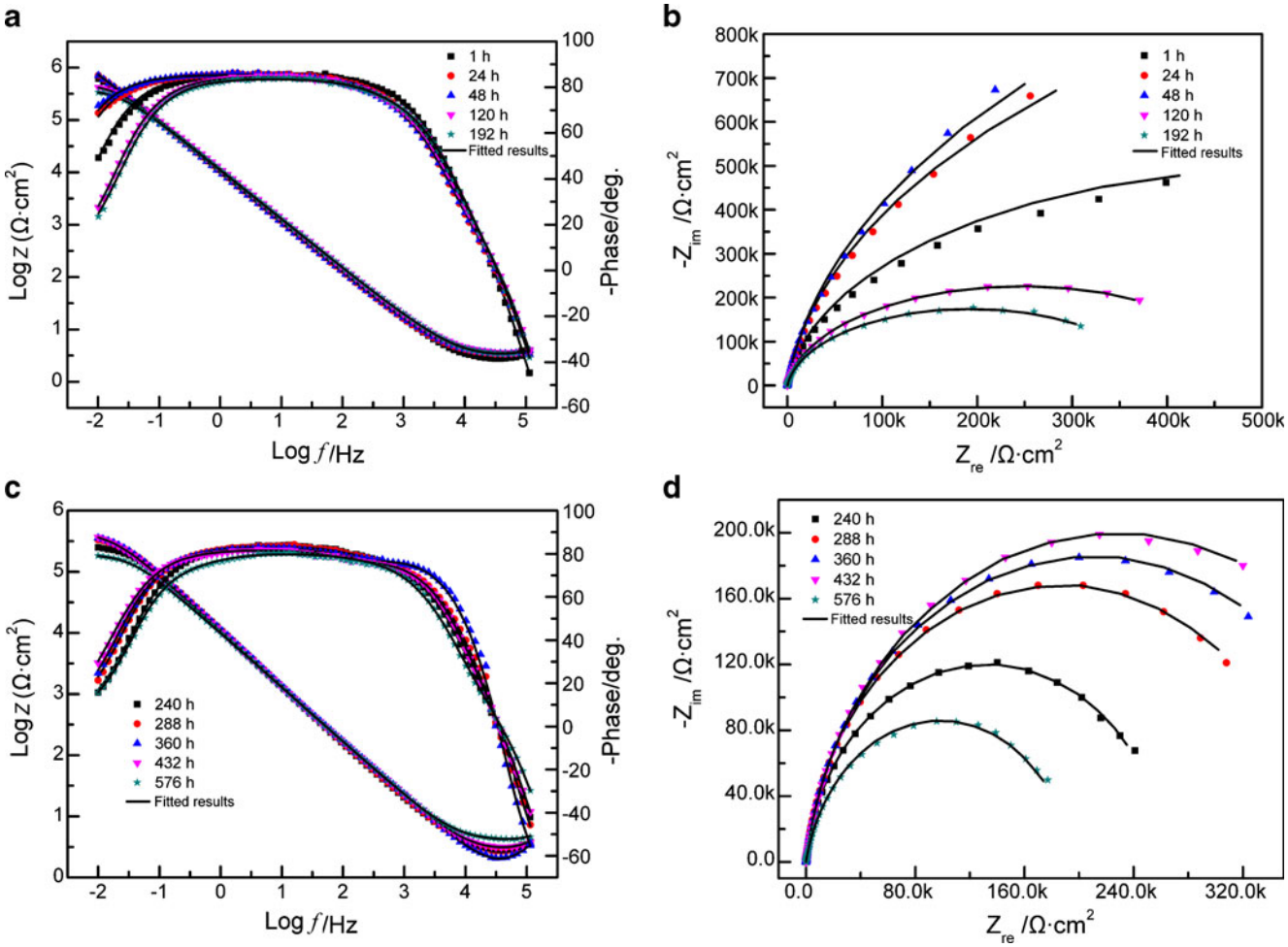

Fig. 6 Electrochemical impedance spectroscopy plots of Ni–Co alloy coating with different immersion times

circuit combinations are used to represent the electrochemical activities of the passive film and the film/solutions interface [34–37]. In Fig. 7, R_{ct} and constant phase element (CPE_1) are the charge transfer resistance and the double layer capacitance. R_f and CPE_2 are the film resistance and the film capacitance, or the resistance and capacitance of the space charge layer. The time constant at high-frequency range originated from the $R_{ct}CPE_1$ combination, while at low-frequency range, initiated from the R_fCPE_2 combination. A *CPE* replaced the capacitance of the double layer (C_{dl}) due to the roughness and inhomogeneity of the electrode surface as reported elsewhere [32]. The impedance of *CPE* is given by the following equation [32]:

$$Z_{\mathrm{CPE}}(\omega) = Y_0^{-1}(j\omega)^{-n} \tag{1}$$

where Y_0 is a constant that is independent of frequency, ω is the angular frequency, $j = \sqrt{-1}$, and n is the exponential index which represents a dispersion of relaxation. When n equals 1, *CPE* represents an ideal capacitor; when n equals 0, *CPE* acts as a pure resistor.

The mathematic expression of the impedance of the electrode system can be described by the following equation [32]:

$$Z(\omega) = j\omega L + R_s + \frac{1}{1/R_{ct} + Y_{01}(j\omega)^{n1}} + \frac{1}{1/R_f + Y_{02}(j\omega)^{n2}} \tag{2}$$

where ω is the angular frequency, and $\omega = 2\pi f$. The calculated equivalent circuit parameters for Ni–Co alloy coating with different immersion times are presented in

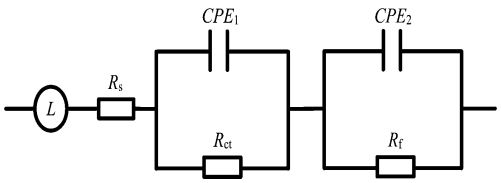

Fig. 7 Electrochemical equivalent circuits used for fitting the experimental data of Ni–Co alloy coating

Table 2 Electrochemical equivalent circuit parameters for Ni–Co alloy coating with different immersion times in neutral 3.5 wt.% NaCl solutions

Immersion time	L (H cm^2)	R_s (Ω cm^2)	R_{ct} (Ω cm^2)	Y_{01} (Ω^{-1} cm^{-2} s^{-n})	n_1	R_f (Ω cm^2)	Y_{02} (Ω^{-1} cm^{-2} s^{-n})	n_2
1 h	4.0×10^{-6}	2.6	1.2	2.52×10^{-3}	0.61	1.1×10^{6}	1.63×10^{-5}	0.95
24 h	3.8×10^{-6}	3.1	3.6	2.88×10^{-5}	0.56	2.3×10^{6}	1.72×10^{-5}	0.95
48 h	3.8×10^{-6}	3.3	5.5	8.33×10^{-4}	0.67	2.8×10^{6}	1.75×10^{-5}	0.95
120 h	3.9×10^{-6}	3.4	5.4	1.29×10^{-3}	0.62	4.9×10^{5}	1.54×10^{-5}	0.95
192 h	4.0×10^{-6}	3.2	4.7	9.01×10^{-4}	0.73	3.9×10^{5}	1.64×10^{-5}	0.94
240 h	4.0×10^{-6}	2.9	7.7	5.98×10^{-4}	0.72	2.6×10^{5}	1.59×10^{-5}	0.94
288 h	4.1×10^{-6}	2.4	9.1	4.35×10^{-4}	0.73	3.7×10^{5}	1.58×10^{-5}	0.93
360 h	4.3×10^{-6}	1.9	12.6	1.03×10^{-4}	0.89	4.2×10^{5}	1.61×10^{-5}	0.93
432 h	3.9×10^{-6}	2.9	13.9	1.75×10^{-4}	0.85	4.6×10^{5}	1.74×10^{-5}	0.92
576 h	3.8×10^{-6}	4.0	7,241.0	1.01×10^{-4}	0.79	1.9×10^{5}	2.18×10^{-5}	0.94

Table 2. The passive film resistance, R_f, increased with the increase of immersion time and reached the maximum of 2.8×10^6 Ω cm^2 with the immersion time of 48 h, and then began to fluctuate. After the immersion time of 576 h, the passive film resistance, R_f, remained 1.9×10^5 Ω cm^2, indicating the good corrosion protection properties. In addition, according to the following equation [39]:

$$C = \varepsilon\varepsilon^o/d \tag{3}$$

where ε is the dielectric constant, ε^o is the permittivity of free space, and d is the thickness of the passive film. A decrease in the capacitance (C) may result from either an increase in the film thickness or a decrease in the dielectric constant. A decrease in the dielectric constant was consistent with a decrease in the defect density within the passive film [39]. Within the course of immersion test, the changes in the capacitance (C), accompanied by a fluctuation in film resistance R_f, may result from the different variational extent in the film thickness and defect density.

Figure 8 shows the surface morphologies of the Ni–Co alloy coating immersed in neutral 3.5 wt.% NaCl solutions for 576 h. Comparing Fig. 2b with Fig. 8, it is clear that surface morphologies variation of the Ni–Co alloy coating, before and after an immersion test, was not obvious. There was no obvious pitting on the surface of Ni–Co alloy coating. According to the EDS analysis results, Fe, Nd, and B elements were not detected on the coating surface. Taking into account the changes of typical EIS plots (shown in Fig. 6a–d) and EDS results after immersion test, it may be safely concluded that the corrosion process did not reach the surface of NdFeB magnet after 576 h immersion test, suggesting the excellent protective properties of the Ni–Co alloy coating for NdFeB magnet in neutral 3.5 wt.% NaCl solutions. As to the pure nickel coating, when the immersion time was 144 h, the macroscopic pitting on the surface of pure nickel coating and the brown rust in solutions were observed, which could be the obvious evidence that the disappearance of the corrosion protection properties, so the images of the corroded coating surface of pure nickel coating were not shown.

From the impedance analysis mentioned above, it can be seen that at the initial stage of immersion test, the impedance values of pure nickel coating and Ni–Co alloy coating were both tremendously higher compared with that of the bare NdFeB magnet indicating the good corrosion protection properties. Ni–Co alloy coating still exhibited excellent anticorrosive properties with the impedance value of 1.9×10^5 Ω cm^2 when the immersion time was 576 h, but corrosion protection properties of nickel coating for NdFeB magnet practically disappeared with the immersion time of 144 h, which suggested that Ni–Co alloy coating could provide longer corrosion protection for sintered NdFeB magnet compared with pure nickel coating. The rapid degeneration in the corrosion protection properties of pure

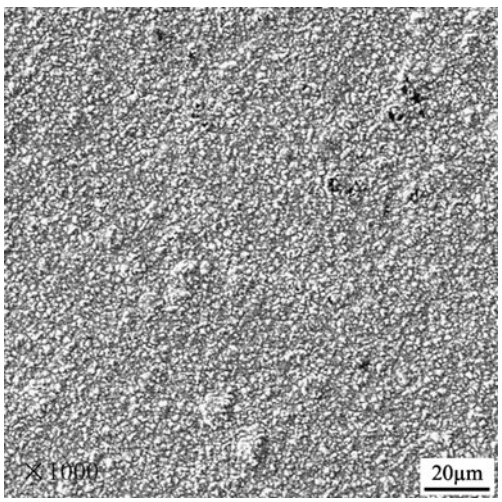

Fig. 8 Surface morphologies of the Ni–Co alloy coating with the immersion time of 576 h

nickel coating for sintered NdFeB magnet was attributed to the inhibiting effect of chloride ions on the formation of passive film formed on its surface and then a non-uniform dissolution of the pure nickel coating [36, 40, 41]. The long-term immersion test indicated that the passive film formed on the surface of Ni–Co alloy coating had high stability, which may be an indicator of the feasibility of the long-term corrosion protection for NdFeB magnet.

Conclusions

In summary, the following conclusions can be drawn from the present investigation.

1. The Ni–Co alloy coating, which exhibited excellent anticorrosive properties, was successfully prepared on the NdFeB magnet.
2. The results of XRD analysis showed that the phase structure of Ni–Co alloy coating was a single solid solution, and the addition of Co in matrix metal Ni changed the preferential orientation from (2 0 0) crystal face for pure nickel coating to (1 1 1) crystal face for Ni–Co alloy coating.
3. The results of SEM analysis revealed that Ni–Co alloy coating exhibited more uniform and compact surface morphologies in comparison to pure nickel coating.
4. The electrochemical corrosion tests indicated that in comparison to pure nickel coating, Ni–Co alloy coating exhibited better anticorrosive properties and could provide long-term good corrosion protection for NdFeB magnet in neutral 3.5 wt.% NaCl solutions.

Acknowledgments The authors acknowledge with thanks the financial supports granted by the Natural Science Foundation of Chongqing, China (CSTC. 2005BB4055), and the High-Tech Cultivation Program of Southwest Normal University (No. XSGX06).

References

1. Matsuura Y (2006) J Magn Magn Mater 303:344
2. Bai G, Gao RW, Sun Y, Han GB, Wang B (2007) J Magn Magn Mater 308:20
3. Vial F, Joly F, Nevalainen E, Sagawa M, Hiraga K, Park KT (2002) J Magn Magn Mater 242–245:1329
4. Cygan DF, McNallanm MJ (1995) J Magn Magn Mater 139:131
5. Rada M, Gebert A, Mazilu I, Khlopkov K, Gutfleisch O, Schultz L, Rodewald W (2006) J Alloys Compd 415:111
6. Yu LQ, Wen YH, Yan M (2004) J Magn Magn Mater 283:353
7. Walton A, Speight JD, Williams AJ, Harris IR (2000) J Alloys Compd 306:253
8. El–Moneim AA, Gebert A, Uhlemann M, Gutfleisch O, Schultz L (2002) Corros Sci 44:1857
9. Saliba–Silva A, Faria RN, Baker MA, Costa I (2004) Surf Coat Technol 185:321
10. Tamborim Takeuchi SM, Azambuja DS, Costa I (2006) Surf Coat Technol 201:3670
11. Man HH, Man HC, Leung LK (1996) J Magn Magn Mater 152:40
12. Cheng CW, Cheng FT (1998) J Appl Phys 83:6417
13. Tamborim Takeuchi SM, Azambuja DS, Saliba–Silva AM, Costa I (2006) Surf Coat Technol 200:6826
14. Hu JM, Liu XL, Zhang JQ, Cao CN (2006) Prog Org Coat 55:388
15. Song L, Wang Y, Lin W, Liu Q (2008) Surf Coat Technol 202:5146
16. Ma CB, Gao FH, Zhang Z, Zhang JQ (2006) Appl Surf Sci 253:2251
17. Hodgson SNB, Hoggarth GG, Davies HA, Buckley RA (1999) J Mater Process Technol 92–93:518
18. Yang XK, Li Q, Hu JY, Zhong XK, Zhang SY (2010) J Appl Electrochem 40:39
19. Yan M, Ying HG, Ma TY (2009) Mater Chem Phys 113:764
20. Zhang H, Song YW, Song ZL (2008) Mater Corros 59:324
21. Tury B, Lakatos-Varsányi M, Roy S (2006) Surf Coat Technol 200:6713
22. Barbosa MR, Gassa LM, Ruiz ER (2001) J Solid State Electrochem 6:1
23. Rozik R, Oriňàková R, Markušová K, Trnková L (2006) J Solid State Electrochem 10:423
24. Oriňáková R, Wiemhöfer H, Paulsdorf J, Barinková V, Bednáriková A, Smith RM (2006) J Solid State Electrochem 10:458
25. Oriňáková R, Oriňák A, Vering G, Talian I, Smith RM, Arlinghaus HF (2008) Thin Solid Films 516:3045
26. Li YD, Jiang H, Huang WH, Tian H (2008) Appl Surf Sci 254:6865
27. Wang GF, Chan KC, Zhang KF (2006) Scripta Mater 54:765
28. Hibbard GD, Aust KT, Erb U (2006) Mater Sci Eng A 433:195
29. Hansal WEG, Tury B, Halmdienst M, Varsányi ML, Kautek W (2006) Electrochim Acta 52:1145
30. Tury B, Lakatos-Varsányi M, Roy S (2007) Appl Surf Sci 253:3103
31. Srivastava M, Ezhil Selvi V, William Grips VK, Rajam KS (2006) Surf Coat Technol 201:3051
32. Cao CN, Zhang JQ (2002) An introduction to electrochemical impedance spectroscopy. Science Press, Beijing
33. Lodhi ZF, Mol JMC, Hovestad A, 't Hoen–Velterop L, Terryn H, de Wit JHW (2009) Surf Coat Technol 203:1415
34. Badawy WA, El–Sherif RM, Shehata H (2009) Electrochim Acta 54:4501
35. Ge HH, Zhou GD, Wu WQ (2003) Appl Surf Sci 211:321
36. Badawy WA, Ismail KM, Fathi AM (2005) Electrochim Acta 50:3603
37. Girault P, Grosseau–Poussard JL, Dinhut JF, Marechal L (2001) Nucl Instr And Meth B 174:439
38. Gaberscek M, Pejovnik S (1996) Electrochim Acta 41:1137
39. Lloyd AC, Noël JJ, McIntyref NS, Shoesmith DW (2005) JOM–J Min 57:31
40. Barbosa MR, Bastos JA, García–Jareño JJ, Vicente F (1998) Electrochim Acta 44:957
41. Nelson JC, Oriani RA (1992) Electrochim Acta 37:2051